P H Y S I C A L   R E V I E W   L E T T E R S

Spin-Transfer Torques in Antiferromagnetic Metals from First Principles

Yuan Xu, Shuai Wang, and Ke Xia

State Key Laboratory for Surface Physics, Institute of Physics, Chinese Academy of Sciences, P.O. Box 603, Beijing 100080, China
(Received 15 August 2007; published 3 June 2008)

In spite of the absence of a macroscopic magnetic moment, an antiferromagnet is spin-polarized on an atomic scale. The electric current passing through a conducting antiferromagnet is polarized as well, leading to spin-transfer torques when the order parameter is textured, such as in antiferromagnetic noncollinear spin valves and domain walls. We report a first principles study on the electronic transport properties of antiferromagnetic systems. The current-induced spin torques acting on the magnetic moments are comparable with those in conventional ferromagnetic materials, leading to measurable angular resistances and current-induced magnetization dynamics. In contrast to ferromagnets, spin torques in antiferromagnets are very nonlocal. The torques acting far away from the center of an antiferromagnetic domain wall should facilitate current-induced domain wall motion.

Antiferromagnet metals (AFMs) are widely used to pin and exchange-bias ferromagnets in devices such as magnetic spin valve read heads [1,2]. The absence of magnetic stray fields makes them very useful as probe tips in spin-polarized scanning tunneling microscopes [3]. AFMs are materials with spontaneous magnetization below a critical Néel temperature at which the magnetic moments of two (or more) sublattices point into opposite directions, such that the net magnetic moment of the AFM vanishes. External magnetic fields cannot be used to manipulate the strongly coupled magnetic moments of AFMs. An alternative for magnetic fields to excite ferromagnets (FMs) is the current-induced spin-transfer torque (STT) [4]. Since the electric current is spin-polarized on an atomic scale, the STT phenomenon may excite the antiferromagnetic order parameter. It is not obvious whether the STT is strong enough and how different sublattices are affected.

Recent theoretical studies [5–7] predicted that, in spin valves with uncompensated antiferromagnets, an angular resistance (AR) effect can be expected. Reversal of the antiferromagnetic order parameter is equivalent with a phase shift by a half period. Furthermore, STT is not an interface effect as in ferrromagnets but effective over the whole AFM. Very recently, strong experimental evidence of STT between AFM and FM has been reported [8]. In addition, the resistance of antiferromagnetic domain walls (AFDWs) in chromium has been measured [9].

In contrast to FMs, AFMs have much smaller shape anisotropies which makes manipulation of its magnetic moments easier—provided one can apply a *sizable* spin torque on the moments. What is the magnitude of the spin torque for an atomic scale spin polarization? Can an atomic scale spin polarization give rise to an observable AR effect? These are the questions that we attempt to answer in this work.

γ-FeMn is an AFM used as a pinning layer in spin valves, and we demonstrate that an electric current can induce angular momentum transfer between magnetic mo-

ments in AFMs. By a detailed analysis of the current and nonequilibrium charge densities, we show that an atomic scale spin polarization exists even for compensated AFMs. A sizable AR is predicted in antiferromagnetic spin valves (AFSVs). In an AFDW, the spin torque is effective not only around the domain wall center but throughout the entire AFM, which can be understood by the suppressed spin precession.

In our calculations, the atomic potential was determined in the framework of the tight-binding (TB) linear muffin-tin-orbital (MTO) method based on density functional theory in the local density approximation [10] and an exchange-correlation potential parametrized by von Barth and Hedin [11]. The self-consistent crystal potentials were used as input to a TB-MTO wave-function-matching calculation, and the scattering wave functions of the whole system were obtained explicitly [12]. To model noncollinear magnetic configurations in AFDWs, a rigid potential approximation is applied, which is a good approximation for sufficiently wide domain walls [13].

The spin current and charge density can be calculated from the scattering wave functions. The torques acting on an atomic plane are defined as the difference between incoming and outgoing spin current [14]. Finally, we focus on transport along the direction perpendicular to the plane fcc(111) as illustrated in Fig. 1(b), where four atoms con-
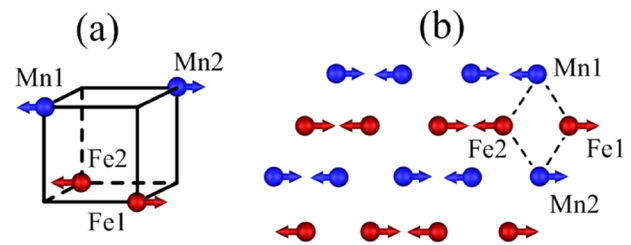

FIG. 1 (color online). (a) Magnetic structure of γ-FeMn. (b) fcc(111) plane of γ-FeMn, where the dashed lines connect the atoms in a unit cell.

226602-1

nected by the dashed lines form a unit cell. fcc(111) is a compensated plane with zero net magnetic moment in each layer.

The magnetic structure of γ-FeMn is shown in Fig. 1(a). This configuration has been observed experimentally [15] and confirmed to be energetically favorable by *ab initio* calculation [16]. There are four inequivalent atoms in a unit cell. The magnetic moments of Fe2 and Mn1 and those of Fe1 and Mn2 point in opposite directions. Our calculation [17] yields the magnetic moments as $m_{\text{Fe}} = 1.4\mu_B$ and $m_{\text{Mn}} = 1.9\mu_B$.

When a current passes through an antiferromagnetic material, the current-induced nonequilibrium charge density integrated over the atomic sphere of an atom is spin-polarized. We define the polarization of atom α as $P_S^\alpha = (\rho_\uparrow^\alpha - \rho_\downarrow^\alpha)/(\rho_\uparrow^\alpha + \rho_\downarrow^\alpha)$, where $\rho_{\uparrow(\downarrow)}^\alpha$ is the spin-resolved nonequilibrium charge density. $\uparrow$ ($\downarrow$) indicates the electron spin parallel (antiparallel) to the spin quantization axis.

In Fig. 2, we plot P_S^α for a single FeMn|Cu interface. We group the system into four inequivalent sublattices according to the inequivalent atoms in the unit cell of γ-FeMn. A nonzero polarization is found even at the Cu side. The sum of the spin polarizations of the four sublattices vanishes in each layer. These results show that a compensated antiferromagnet injects a spin polarization into a normal metal that oscillates on an atomic scale.

Let us consider now an AFSV denoted as FeMn1(θ)|Cu|FeMn2|Cu, where an infinitely thick FeMn1 serves as the fixed layer and FeMn2 as the free layer. The z axis of spin space is set along the magnetization of the free layer, and θ gives the relative angle between both order parameters. In our calculations, the thicknesses

of the Cu spacer and the FeMn2 free layer are chosen to be both 10 monolayers (ML) [18].

The top panel in Fig. 3 illustrates the magnetic structure of the so-called parallel configuration ($\theta = 0°$). Here and in the following, we group the four sublattices into two according to the direction of their magnetic moments. When the magnetization of FeMn1 is rotated from $\theta = 0°$ to $\theta = 180°$ (the antiparallel configuration), the electric resistance changes.

The bottom panel in Fig. 3 gives the spin-polarized current at the two sublattices. When the magnetizations of the two AFM layers are collinear, there is no net current spin polarization. However, the spatial distribution of spin-polarized current is not trivial. In fact, the spin-polarized currents on the two sublattices do not vanish even in Cu. They are identical in magnitude but oppositely spin-polarized. Another finding is that the spin-polarized current oscillates between the two sublattices and is not conserved within one sublattice.

The AR ratio in terms of conductance as $[G(0°) - G(180°)]/G(180°)$ amounts to a measurable 5%. The remaining question is the robustness of this AR effect in the presence of interfacial disorder. We modeled disorder by an interfacial alloy with a lateral supercell method [12]. For a 1 ML (FeMn)$_{1-x}$Cu$_x$ interfacial alloy, the AR dependence on interfacial alloy concentration x is shown in Fig. 4, which indicates that the AR is somewhat suppressed in the presence of disorder but should remain to be observable.

It is interesting to investigate the STT due to the atomic scale spin-dependent scattering. Before going into the numerical results, we analyze the symmetry of the STT. For one sublattice, similar to that of FM, the torque on a local magnetic moment $\mathbf{m}$ is proportional to $\mathbf{m} \times \mathbf{M} \times \mathbf{m}$
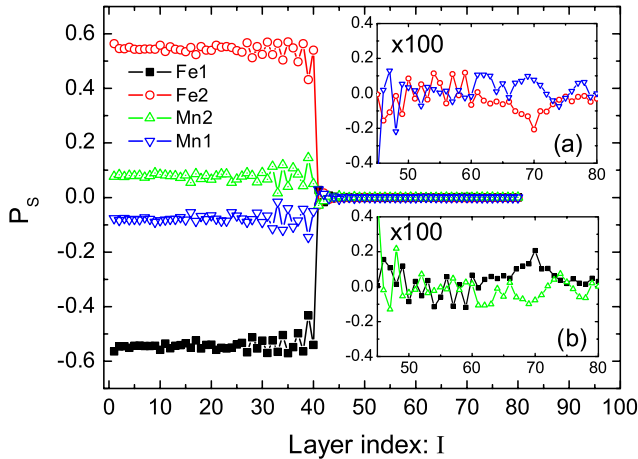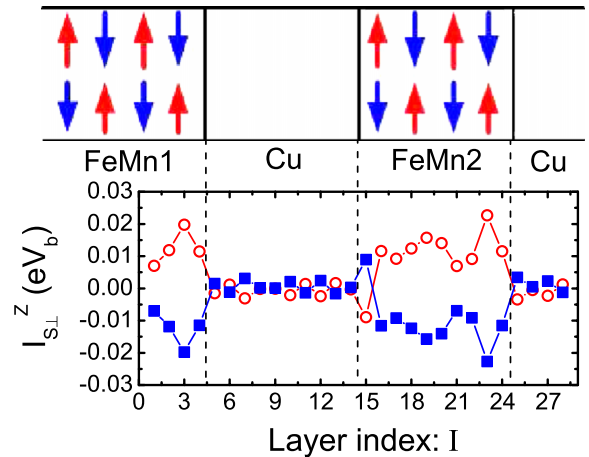

FIG. 2 (color online). Layer-resolved spin polarization of nonequilibrium charge density P_S^α on the four inequivalent sublattices of the FeMn|Cu system, where FeMn occupies the 1st–40th layers and Cu the 41st–80th layers. The electron current flows from FeMn to Cu. Inset (a) gives the P_S on the Cu side for the inequivalent sublattices corresponding to Fe2 and Mn1. Inset (b) gives the P_S on the Cu side for the inequivalent sublattices corresponding to Fe1 and Mn2.

FIG. 3 (color online). Top panel: Cartoon of the parallel configuration $\theta = 0°$ of an AFSV. The red and blue arrows denote the two sublattices A and B, respectively. Bottom panel: The layer-resolved z component of spin-polarized current $I_{s\perp}^z$, where the subscript $\perp$ denotes the current perpendicular to the fcc(111) plane and the red circles (blue squares) represent the spin-polarized current on the sublattice A (B).
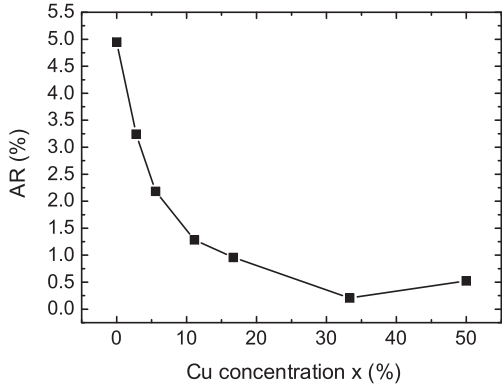
FIG. 4.   Cu concentration x dependence of AR in the system FeMn1|Cu(10ML)|FeMn2(10ML)|Cu.

(in-plane) and $\mathbf{m} \times \mathbf{M}$ (out-of-plane), where $\mathbf{M}$ denotes the source of spin current. For another sublattice, both $\mathbf{m}$ and $\mathbf{M}$ are reversed. The in-plane torque is also reversed, whereas the out-of-plane torque remains unchanged. Because the in-plane torque $\mathbf{T}_\parallel$ on two sublattices is identical in magnitude and opposite in direction and the magnetization of two sublattices points in opposite directions, the net effect of STT tends to rotate those moments to-
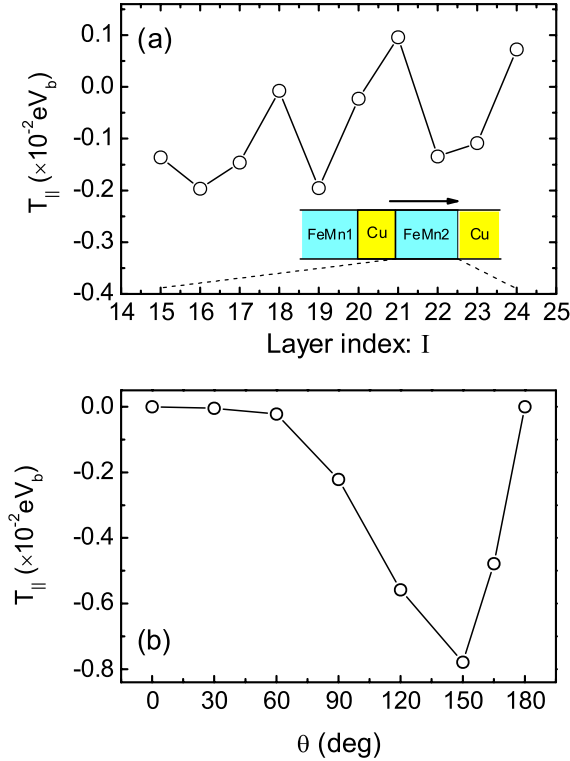
gether. In contrast to $\mathbf{T}_\parallel$, the out-of-plane torque $\mathbf{T}_\perp$ acts identically on the two magnetic sublattices. As the exchange coupling in the AFM is strong, out-of-plane torques will not result in any significant effect on the dynamics of the magnetic moments.

As shown in Fig. 5(a), the spin torque in the AFM layer oscillates deep into material which differs from a conventional FM spin valve [19,20]. The angular dependence of the total in-plane torque acting on a sublattice (Fe1&Mn2) in FeMn2 is shown in Fig. 5(b). For $\theta = 150°$, the torque $(4.1 \times 10^{-4}\ \mathrm{eV}_b/\mu_B)$ acting on the surface atoms is much smaller than that in a FM spin valve $(\sim 10^{-3}\ \mathrm{eV}_b/\mu_B)$ [21]. However, due to the slow decay of the spin torque in AFMs, the integrated torque on per atom of AFMs $(2.4 \times 10^{-4}\ \mathrm{eV}_b/\mu_B)$ is comparable to that in FMs.

A similar spin-transfer effect should occur in AFDWs. As domain wall physics in AFMs has not been fully understood [22], we simply consider a Bloch-like domain wall which could exist in the experiment [23], as shown in Fig. 6(a). The configuration is described by $\theta(y) = \frac{\pi}{2} + \arcsin[\tanh(\frac{y-y_0}{\lambda_{DW}})]$, where λ_{DW} is the characteristic length which is selected to be 4 ML and y_0 the center of the wall. The spin direction in each monolayer along the wall is shown in Fig. 6(b). The change of the total conductance due to the formation of a wall is 2.8% for a 4 ML thick

FIG. 5 (color online). (a) The layer-resolved in-plane torque $T_\parallel$ on one sublattice (Fe1&Mn2) of FeMn2 in FeMn1(θ)|Cu(10ML)|FeMn2(10ML)|Cu, as shown by the cartoon. Here $\theta = 150°$, electrons flow from FeMn1 to FeMn2, and FeMn2 is located at $15 \leq I \leq 24$. (b) Angular dependence of the in-plane torque $T_\parallel$ on the sublattice (Fe1&Mn2) of FeMn2 in the same system.
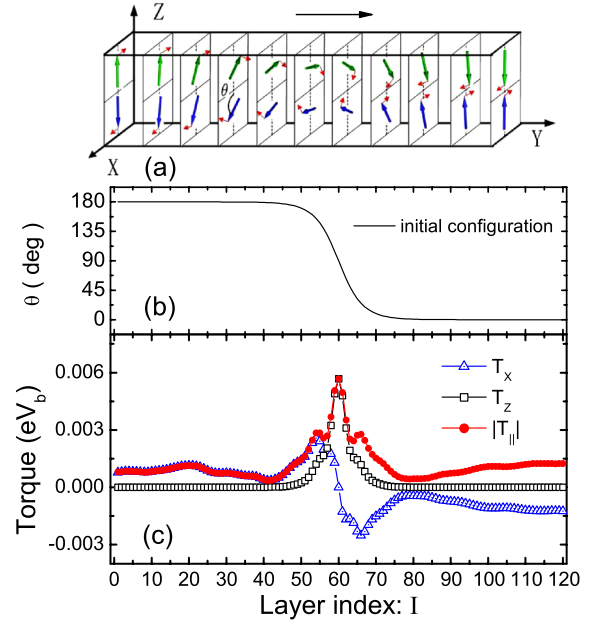

FIG. 6 (color online).   (a) Schematic view of the AFDW, in which two sublattices are indicated by the green and blue arrows, the magnetization is rotated in the plane by an angle θ, and the electrons are injected from the left side. The in-plane torque directions are indicated by the red arrows. (b) θ as the function of position. (c) Spin torques acting on the sublattice (Fe1&Mn2) in each monolayer with initial configuration, where T_X and T_Z denote the in-plane components and $|T_\parallel|$ is the absolute value of in-plane torques.

domain wall, which is comparable to that in a FM with the same width.

Figure 6(c) shows the in-plane torque exerted on one sublattice (Fe1&Mn2) as a function of position in the domain wall. There is a substantial STT in the region far away from the domain wall center. This is attributed to the spin degeneracy of the electronic band structure in the AFM. The injected spin can penetrate and precess coherently until deep into the AFM. As a result, STT in AFM is very nonlocal, at least in the absence of disorder scattering.

We investigate the dynamics of the AFDW with the Landau-Lifshitz-Gilbert (LLG) equation [24] by using our calculated STT. An AFM with two sublattices is described by two sets of coupled LLG equations. Here we decouple the equations by assuming that the magnetizations of two sublattices in the same layer are antiparallel to each other at any time. This should be reasonable due to a strong antiferromagnetic coupling between the two sublattices.

To investigate dynamics of the domain wall in the presence of a current, we follow the method of Ohe and Kramer [25], who studied FM domain walls. This method consists of several steps: (i) Given a domain wall configuration, we calculate the STT acting on each site under a certain current density; (ii) the obtained spin torque at each site is substituted into the LLG equation to obtain a set of equations for each site in the domain wall at a given time t; (iii) by integrating the LLG equation, we obtain the domain wall configuration after an interval at $t' = t + \delta t$; (iv) once a new domain wall configuration is obtained, we can calculate the STT again, and the process is repeated. The interval δt between two consecutive steps is chosen small enough to guarantee numerical convergence of the solution.

In particular, a magnetic anisotropy constant of 1.35×10^5 erg/cm^3, exchange stiffness constant of 0.94×10^{-9} erg/cm, magnetization of sublattice of 650 G, and Gilbert damping constant of 0.1 are used in our calculation.

Under a current density of 5×10^7 A/cm^2 and starting from the initial domain wall configuration mentioned above, we obtained results for 10 time steps of $\delta t = 2$ ps. The domain wall moves in the $-Y$ direction, and the estimated velocity is 4 m/s. In contrast to the FM domain wall, the velocity is maintained due to the vanishing demagnetization field. For the same reason, when no pinning field is taken into account, the critical current that sets the AFDW into motion is also expected to be very small as compared to a FM domain wall.

In summary, we find an atomic scale spin polarization in completely compensated AFMs. An STT can be induced by an electric bias. In AFSVs, a sizable AR is predicted, and the STT is found to be comparable to that in conventional FM spin valves. In AFDWs, the torques turn out to be nonlocal. The spin dynamics of AFDWs is studied by including the STT in the LLG equation for AFMs.

[1] W. H. Meiklejohn and C. P. Bean, Phys. Rev. **102**, 1413 (1956).
[2] J. Bass, A. Sharma, Z. Wei, and M. Tsoi, J. Magnetics **13**, 1 (2008).
[3] A. Kubetzka *et al.*, Phys. Rev. Lett. **88**, 057201 (2002).
[4] J. C. Slonczewski, J. Magn. Magn. Mater. **159**, L1 (1996); L. Berger, Phys. Rev. B **54**, 9353 (1996); J. A. Katine *et al.*, Phys. Rev. Lett. **84**, 3149 (2000); X. Waintal *et al.*, Phys. Rev. B **62**, 12 317 (2000); J. Z. Sun, J. Magn. Magn. Mater. **202**, 157 (1999); M. Tsoi *et al.*, Phys. Rev. Lett. **80**, 4281 (1998).
[5] A. S. Núñez *et al.*, Phys. Rev. B **73**, 214426 (2006).
[6] R. A. Duine *et al.*, Phys. Rev. B **75**, 014433 (2007).
[7] P. Haney *et al.*, Phys. Rev. B **75**, 174428 (2007).
[8] Z. Wei *et al.*, Phys. Rev. Lett. **98**, 116603 (2007).
[9] R. Jaramillo *et al.*, Phys. Rev. Lett. **98**, 117206 (2007).
[10] I. Turek *et al.*, *Electronic Structure of Disordered Alloys, Surfaces and Interfaces* (Kluwer, Boston, 1997).
[11] U. von Barth and L. Hedin, J. Phys. C **5**, 1629 (1972).
[12] K. Xia *et al.*, Phys. Rev. B **73**, 064420 (2006).
[13] Self-consistent calculations show that when the relative angle between neighboring magnetic atoms is less than 20°, magnetic moments change less than 2%.
[14] S. Wang, Y. Xu, and K. Xia, Phys. Rev. B **77**, 184430 (2008).
[15] J. S. Kouvel and J. S. Kasper, J. Phys. Chem. Solids **24**, 529 (1963); P. Bisanti, G. Mazzone, and F. Sacchetti, J. Phys. F **17**, 1425 (1987).
[16] D. Spišák and J. Hafner, Phys. Rev. B **61**, 11 569 (2000).
[17] The Wigner-Seitz radii of the two atoms satisfy $r_{Fe}/r_{Mn} = 0.98$. We use a grid of 57 600 $k_\parallel$ points in the full two-dimensional Brillouin zone for the transport calculations.
[18] Several relative configurations between the two FeMn (111) planes facing each other across the Cu spacer can be considered. In this work, we take the most convenient one by replacing 10 ML of the bulk FeMn with Cu atoms.
[19] M. D. Stiles *et al.*, Phys. Rev. B **66**, 014407 (2002).
[20] M. Zwierzycki *et al.*, Phys. Rev. B **71**, 064420 (2005).
[21] D. M. Edwards *et al.*, Phys. Rev. B **71**, 054407 (2005).
[22] M. Ando and S. Hosoya, Phys. Rev. Lett. **29**, 281 (1972); F. Nolting *et al.*, Nature (London) **405**, 767 (2000); C. L. Chien *et al.*, Phys. Rev. B **68**, 014418 (2003).
[23] F. Radu and H. Zabel, Springer Tracts Mod. Phys. **227**, 97 (2008).
[24] Z. Li and S. Zhang, Phys. Rev. B **70**, 024417 (2004).
[25] J. Ohe and B. Kramer, Phys. Rev. Lett. **96**, 027204 (2006).